

The onset of the West African monsoon simulated in a high-resolution atmospheric general circulation model with reanalyzed soil moisture fields

T. J. Yamada,^{1*} S. Kanae,² T. Oki³ and Y. Hirabayashi⁴

¹Faculty of Engineering, Hokkaido University, Kita 13, Nishi 8, Kita-ku, Sapporo 060-8628, Japan

²Department of Mechanical and Environmental Informatics, Tokyo Institute of Technology, 2-12-1 O-okayama, Meguro-ku, Tokyo 152-8522, Japan

³Institute of Industrial Science, The University of Tokyo, 4-6-1 Komaba, Meguro-ku, Tokyo 153-8595, Japan

⁴Institute of Engineering Innovation, School of Engineering, The University of Tokyo, 2-11-16 Bunkyo-ku, Tokyo 113-8656, Japan

*Correspondence to:

T. J. Yamada, Faculty of Engineering, Hokkaido University, Kita 13, Nishi 8, Kita-ku, Sapporo 060-8628, Japan.
E-mail: tomohito@eng.hokudai.ac.jp

Abstract

The simulation of the onset of the West African monsoon (WAM), associated with the northward shift of the Intertropical Convergence Zone (ITCZ) occurring in May, June, and July, is a challenging task for atmospheric general circulation models (AGCMs), because of complex water and energy balance through the land-atmosphere interaction as well as atmospheric processes. We provide evidence that a combination of state-of-the-art global fields of reanalyzed soil moisture anomalies and a sufficiently high-resolution (~50 km) AGCM produces a successful simulation of the northward shift of the ITCZ and the following onset of the WAM in July. Copyright © 2011 Royal Meteorological Society

Keywords: West African monsoon; soil moisture; African Easterly Jet; AGCM

Received: 25 June 2011

Revised: 15 September 2011

Accepted: 22 November 2011

1. Introduction

The Sahel is one of the most densely populated regions of the African continent and is characterized meteorologically as a monsoon region. The management of water resources across the Sahel in the monsoon season is important for agriculture and other human activities. The Intertropical Convergence Zone (ITCZ) shifts abruptly northward from a quasi-stationary location at 5°N (Gulf of Guinea) in May–June (MJ) to another quasi-stationary location at 10°N in July–August (JA; Sultan and Janicot, 2000, 2003), bringing about the onset of the monsoon over the Sahel. The monsoon onset is routinely captured in regional model simulations (Gallée *et al.*, 2004; Hagos and Cook, 2007) by realistic lateral boundary conditions of the atmosphere. On the other hand, many GCMs, despite good simulations of the mature West African monsoon (WAM) in August, have failed to accurately simulate the ITCZ rapid northward transition from the Gulf of Guinea (d'Orgeval *et al.*, 2006). This article shows a successful example of the onset simulation in a high-resolution atmospheric general circulation model (AGCM) that is not forced with realistic lateral boundary conditions and atmospheric initial conditions.

2. The model and experimental design

Our study involves two sets of eight AGCM simulations in 1998, using the AGCM designed for the Earth Simulator (AFES; Ohfuchi *et al.*, 2004). The AFES

initially adopted physical and dynamical cores from the Center for Climate System Research (The University of Tokyo)/National Institute for Environmental Studies (CCSR/NIES) AGCM (Numaguti *et al.*, 1997), which were then modified and developed independently at the Earth Simulator Center.

The eight AGCM simulations started at 00Z on 24–31 March using the European Centre for Medium-Range Weather Forecasts (ECMWF) Reanalysis 40 (ERA40) dataset as an atmospheric initial condition. We used a T239 (~50 km) triangular truncation, which is approximately one fifth smaller than the resolutions (250–300 km) used in previous studies (Kanae *et al.*, 2006; Douville *et al.*, 2007). We used the pentad Atmospheric Model Intercomparison Project (AMIP) optimally interpolated Sea Surface Temperature (OISST) data of 1998 as the boundary condition. Hereafter, we refer to the set of basic model simulations as the control run (hereafter CTRL-T239), in which the AMIP OISST data were prescribed at each time step. The eight simulations differed only in their initial atmospheric conditions.

The ensemble mean of the eight simulations is analyzed below. Another set of eight simulations called SOIL-T239 differed from CTRL-T239 only in the treatment of subsurface soil moisture. In CTRL-T239, subsurface soil moisture was computed by modeled precipitation and atmospheric conditions with land–atmosphere interactions, as in the standard in AGCM simulations. Global fields of observation-based soil moisture are not available yet; therefore, in SOIL-T239, a simulated global field of reanalyzed subsurface soil moisture was prescribed at each time

step; this field was produced by an off-line land surface model using ground and satellite-based precipitation observations (Global Precipitation Climatology Project, GPCP) (Huffman *et al.*, 2001) and reanalyzed atmospheric forcing data (Hirabayashi *et al.*, 2005). The design of SOIL-T239 is analogous to those AGCM simulations using observed global SSTs as a boundary condition, such as in studies of the impact of El Niño. We defined subsurface soil moisture as that 5 cm below the land surface. Therefore, the surface soil layer (0–5 cm) freely evolves through land–atmosphere interactions.

3. Results

Upper panels of Figure 1 show the simulated and observed geographical distributions of MJ mean precipitation and horizontal wind vectors at a lower height (925 hPa). The observation (Figure 1(a)) clearly shows the ITCZ over the Gulf of Guinea (2–6°N, 10°W–5°E). On the other hand, CTRL-T239 does not simulate the ITCZ (Figure 1(b)). The precipitation of CTRL-T239 is approximately 3.3 mm/day, as opposed to the observed 7.6 mm/day, with unrealistic southerly flow affecting the Sahel. In contrast, SOIL-T239 successfully simulates the geographical distribution of precipitation (~6.1 mm/day) over the Gulf of Guinea and weakened horizontal wind vectors at 925 hPa over the southern vicinity of the Sahel in MJ (Figure 1(c)). Our results indicate that the geographical pattern and strength of the oceanic ITCZ in the vicinity of the coastline can potentially be improved by incorporating reanalyzed soil moisture anomalies in high-resolution AGCMs through the stationary unstable lower atmosphere during the 2 months.

Lower panels of Figure 1 show the results for July. The ITCZ reaches to the Sahel, making the onset of the WAM (Figure 1(d)). CTRL-T239 (Figure 1(e))

does not have enough precipitation contrary to the observation. SOIL-T239 simulates well the geographical distribution of precipitation in July over many parts of Sahelian countries (Figure 1(f)). In the first half of July, the area of large observed precipitation abruptly shifts northward to 10°N (Figure 2(a)). The poor simulation of CTRL-T239 in July could be a consequence of the ITCZ activity in MJ (Figure 2(b)). Similarly, SOIL-T239 simulates clearly the northward shift of the ITCZ to the Sahel (Figure 2(c)) with sufficient precipitation contrary to CTRL-T239. Comparing the observation (Figure 2(a)) and SOIL-T239 (Figure 2(c)), SOIL-T239 exhibits smoother latitudinal shifts than the observed data due to averaging the results of the eight ensembles. Each ensemble member also represents the abrupt northward shift of the ITCZ.

The main driving forces of the ITCZ propagation northward to the Sahel are the low-level meridional flow (between the surface and 800 hPa) and the African Easterly Jet (AEJ) at 600–700-hPa height in association with the intense solar heating over the Sahara (Druyan and Hall, 1994; Cook, 1999; Sultan and Janicot, 2003). Observations indicate a strong convergence region at 925 hPa over 2–6°N in MJ, which shifts northward to 8–12°N in the first half of July (Figure 2(d)). The observed 700-hPa cyclonic vorticity also shifts between MJ (over the Gulf of Guinea) and July (over the Sahel, Figure 2(g)). Relative vorticity is an indication of the potential to develop barotropic instability, which grows by converting potential energy associated with the mean horizontal temperature gradient, as especially seen in the unstable flank of the AEJ, where the African Easterly Waves (AEWs) can develop (Burpee, 1972; Norquist *et al.*, 1997). The figures show clear northward displacement of the low-level convergence and the cyclonic vorticity, followed by a northward shift of the ITCZ. Low-level convergence in CTRL-T239 differs from the observation,

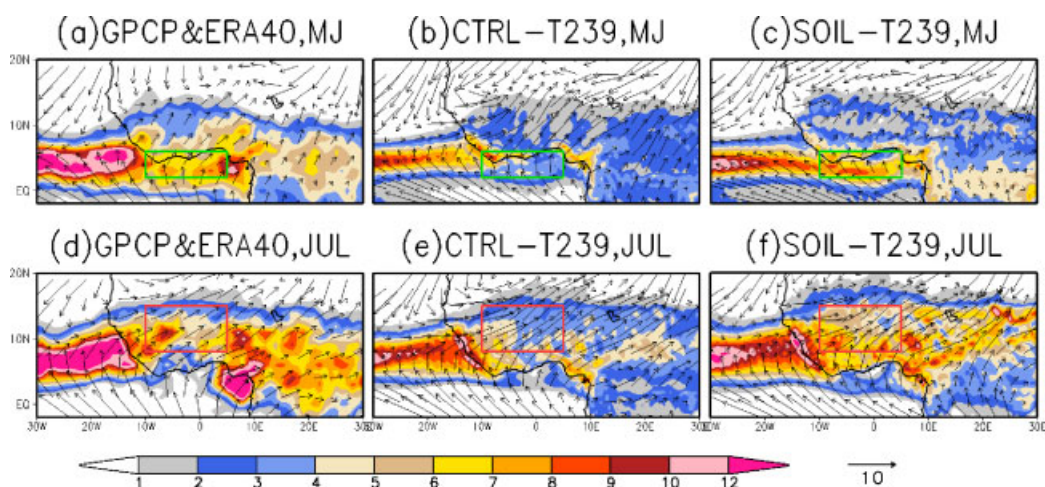


Figure 1. Geographical distributions of precipitation and wind vector at 925 hPa height for GPCP, CTRL-T239, and SOIL-T239. Upper figures are for May and June (MJ) and lower figures are for July. Wind vectors in (a) and (d) were plotted by the European Centre for Medium-Range Weather Forecast (ECMWF) Reanalysis 40 (ERA40) dataset. The difference between the mean MJ daily precipitation between SOIL-T239 (c) and CTRL-T239 (b) satisfied the 99% statistical significance level by Student's *t*-test in and around the Gulf of Guinea. Quadrilateral green (pink) lines indicate the targeted the Gulf of Guinea (the Western Sahel).

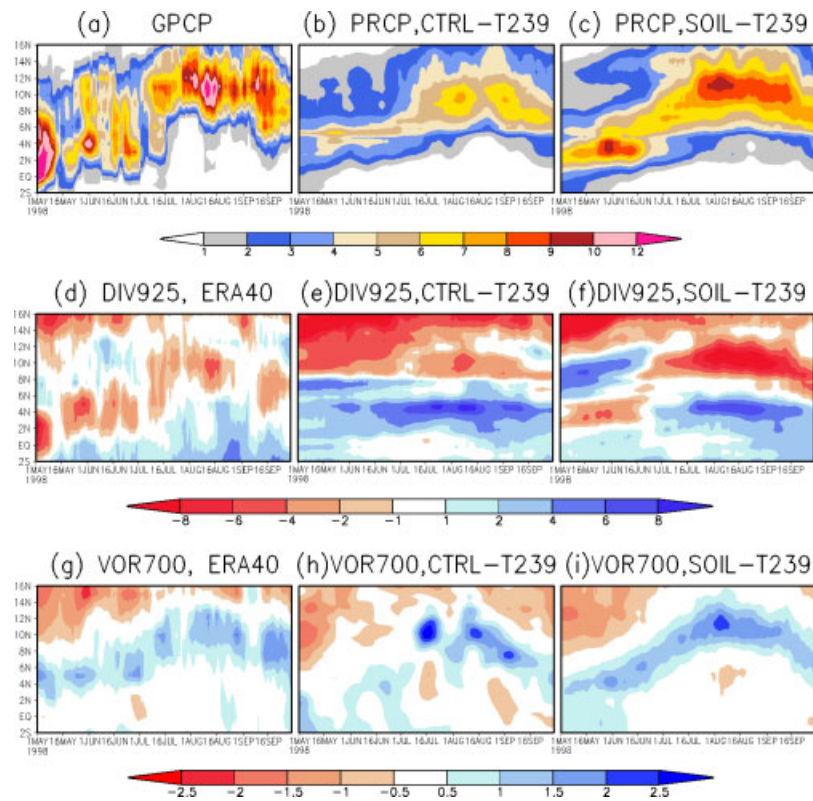


Figure 2. Latitudinal diagrams of 10-day mean precipitation (mm/day) (upper panels), horizontal wind convergence (1/s) at 925 hPa height (middle figures), and relative vorticity (1/s) at 700 hPa height (lower panels) averaged between 10°W and 5°E for GPCP, ERA40, CTRL-T239, and SOIL-T239. The left panels are for GPCP and ERA40; the middle panels are for CTRL-T239; and the right panels are for SOIL-T239. In the middle panels, values are multiplied by 10⁶. Warmer (cooler) colors indicate convergences (divergences). In the lower panels, values are multiplied by 10⁵. Cooler (warmer) colors indicate cyclonic (anticyclonic) disturbance.

and the cyclonic vorticity is not active until mid-July (Figure 2(h)) in the ensemble mean, even though a few of the members intermittently show weaker cyclonic vorticities over the Gulf of Guinea. In contrast, SOIL-T239 simulates both the low-level convergence (Figure 2(f)) and the cyclonic vorticity over the Gulf of Guinea in MJ (Figure 2(i)). Furthermore, a northward shift of these two prominent features from the Gulf of Guinea to the Sahel is simulated in the first half of July (Figure 2(i)). Thus, the combined good simulation of the low-level convergence and the cyclonic vorticity led to the appropriate representation of the onset of the WAM.

To understand why SOIL-T239 reproduces the cyclonically sheared side of the AEJ better than CTRL-T239, we examine the vertical profiles of MJ mean zonal wind velocities averaged between 10°W and 5°E (Figure 3(a)–(c)). Warmer colors in the middle troposphere indicate the AEJ. The meridional location of the AEJ simulated by SOIL-T239 agrees with the observations. In CTRL-T239, strong easterly winds extend to 2°S, and the AEJ formed farther southward compared to the observations. The surface and lower tropospheric warm temperature anomaly, particularly over the Sahel and the Sahara, is caused by reduced release of latent heat and may be one reason in CTRL-T239 for the incorrect location of the AEJ (Figure 3(d)). The reason for the dry bias in CTRL-T239 over the regions could not be assessed

without performing SOIL-T239, because of limited observation. Finally, the same types of experiments have been performed also at lower resolution (T39, ~300 km): SOIL-T39 and CTRL-T39, to discuss the horizontal dependency of the onset of the WAM. The prominent feature of the lower resolutions (Figure 4(a) and (b)) is too much precipitation over the Sahel in MJ contrary to observation (Figure 2(a)). As clearly shown in Figure 4(c)–(f), the low-level convergence and the cyclonic vorticity at 700 hPa over the Gulf of Guinea are also not produced with the lower resolution, despite the realistic soil moisture fields over land. Therefore, such a low resolution is not sufficient to represent the meridional characteristics of atmospheric circulations for the WAM onset.

4. Discussion

Previous studies have mainly discussed how soil moisture anomalies affect the variability in local precipitation predominantly through a one-dimensional land–atmosphere process (Koster *et al.*, 2004). Our study demonstrates that realistic soil moisture states influence precipitation nonlocally by controlling the low-level convergence and conditions for AEWs through the determination of heat low and geostrophic circulation as well as surface hydro-meteorological conditions such as pressure field, the Bowen ratio

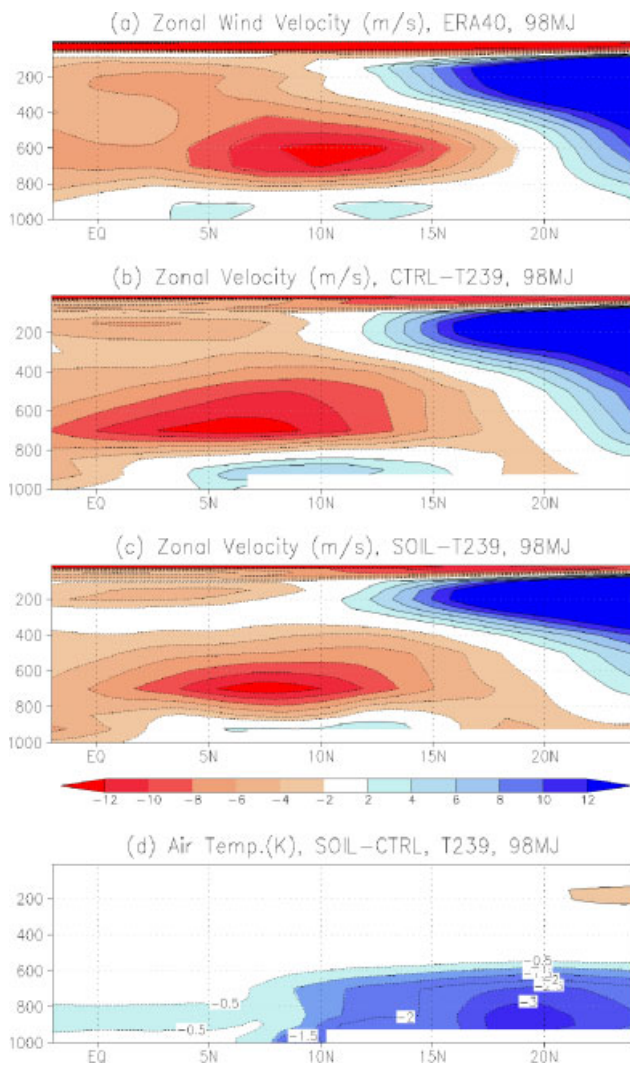


Figure 3. Vertical and meridional distributions of mean May and June (MJ) zonal wind velocity for ERA40 (a), CTRL-T239 (b) and SOIL-T239 (c). (d) Mean MJ air temperature differences between SOIL-T239 and CTRL-T239.

and surface temperature gradient. Cook (1999) demonstrated the connection between soil moisture distributions and the AEJ and the thermal wind relationship during the monsoon's mature stage. Both the strength and the meridional location of the AEJ, which forms the AEWs, were simulated well in SOIL-T239. Our result suggests that this relationship may also be important to simulate the onset. The difference of the initial stage of the WAM between CTRL-T239 and SOIL-T239 further affects the prediction of Atlantic hurricane activity (not shown). One limitation of our study is that computational costs do not allow performing multiyear simulations at this time, which would increase the confidence in the results. This will be the subject of a future article.

From the viewpoint of climate change, the fourth assessment report of the Intergovernmental Panel on Climate Change (IPCC) noted that the Sahel could become marginally more dry based on multi-model assessment (Cook and Vizy, 2006), whereas some

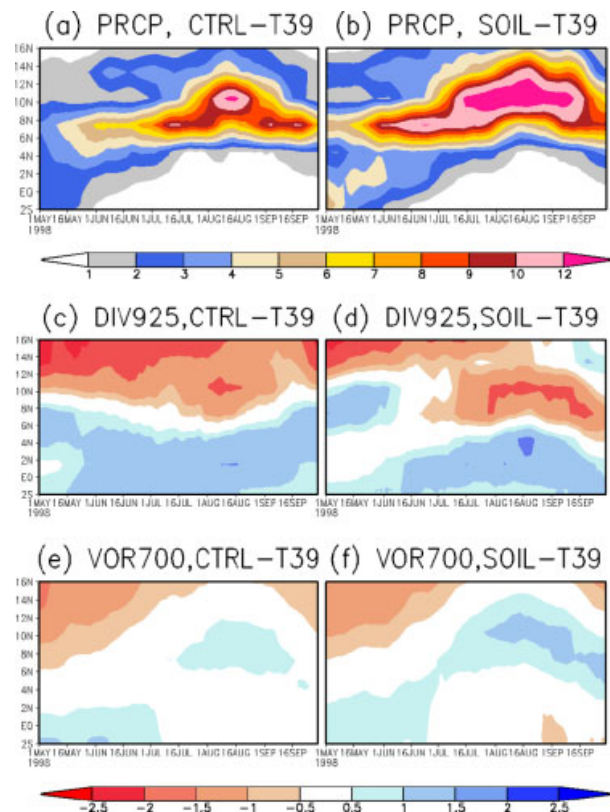


Figure 4. Latitudinal diagrams of 10-day mean precipitation (mm/day), horizontal wind convergence (1/s) at 925 hPa height (upper panels), and relative vorticity (1/s) at 700 hPa height (lower panels) averaged between 10°W and 5°E for CTRL-T39 and SOIL-T39. Details are provided in Figure 2.

individual models have projected an increase in rainfall across the Sahel (Liu *et al.*, 2002). This work implies that the spatial resolution and the degree of land–atmosphere coupling may strongly affect the prediction of the WAM under climate change.

Acknowledgements

The authors wish to express their gratitude to Oreste Reale, Wataru Ohfuchi, Takeshi Enomoto, Akira Kuwano-Yoshida, and Nobumasa Komori for helpful comments and suggestions. All computational resources were provided by the Earth Simulator Center in Japan Agency for Marine-Earth Science and Technology. This work was supported by Core Research for Evolutional Science and Technology, Japan Science and Technology Agency (CREST/JST).

References

- Burpee RW. 1972. The origin and structure of easterly waves in the lower troposphere of North Africa. *Journal of the Atmospheric Sciences* **29**: 77–90.
- Cook KH. 1999. Generation of the African Easterly Jet and its role in determining West African precipitation. *Journal of Climate* **12**: 1165–1184.
- Cook KH, Vizy EK. 2006. Coupled model simulations of the West African monsoon system: twentieth- and twenty-first-century simulations. *Journal of Climate* **19**: 3681–3703.

- d'Orgeval T, Polcher J, Li L. 2006. Uncertainties in modeling future hydrological change over West Africa. *Climate Dynamics* **26**: 93–108.
- Douville H, Conil S, Tyteca S, Voldoire A. 2007. Soil moisture memory and West African monsoon predictability: artefact or reality? *Climate Dynamics* **28**: 723–742.
- Druryan LM, Hall TM. 1994. Studies of African wave disturbances with the GISS GCM. *Journal of Climate* **7**: 261–276.
- Gallée H, Moufouma-Okia W, Bechtold P, Brasseur O, Dupays I, Marbaix P, Messenger C, Ramel R, Lebel T. 2004. A high-resolution simulation of a West African rainy season using a regional climate model. *Journal of Geophysical Research* **109**: D05108. DOI: 10.1029/2003JD004020.
- Hagos SM, Cook KH. 2007. Dynamics of the West African monsoon jump. *Journal of Climate* **20**: 5264–5284.
- Hirabayashi Y, Kanae S, Struthers I, Oki T. 2005. A 100-year (1901–2000) global retrospective estimation of terrestrial water cycle. *Journal of Geophysical Research (Atmosphere)* **110**(D19): DOI: 10.2029/2004JD005492.
- Huffman GJ, Adler RF, Morrissey MM, Bolvin DT, Curtis S, Joyce R, McGavock B, Susskind J. 2001. Global precipitation at one-degree daily resolution from multisatellite observations. *Journal of Hydrometeorology* **2**: 36–50.
- Kanae S, Hirabayashi Y, Yamada T, Oki T. 2006. Influence of “realistic” land-surface wetness on predictability of seasonal precipitation in boreal summer. *Journal of Climate* **19**: 1450–1460.
- Koster RD, Dirmeyer PA, Guo Z, Bonan G, Chan E, Cox P, Gordon CT, Kanae S, Kowalczyk E, Lawrence D, Liu P, Lu CH, Malyshev S, McAvaney B, Mitchell K, Mocko D, Oki T, Oleson K, Pitman A, Sud YC, Taylor CM, Verseghy D, Vasic R, Xue Y, Yamada T. 2004. Regions of coupling between soil moisture and precipitation. *Science* **305**: 1138–1140.
- Liu P, Meehl GA, Wu GX. 2002. Multi-model trends in the Sahara induced by increasing CO₂. *Geophysical Research Letters* **29**: 1881. DOI: 10.1029/2002GL015923.
- Norquist DC, Recker EE, Reed RJ. 1997. The energetics of African wave disturbances as observed during Phase III of GATE. *Monthly Weather Review* **105**: 334–342.
- Numaguti A, Takahashi M, Nakajima T, Sumi A. 1997. Description of CCSR/NIES atmospheric general circulation model. Study on the climate system and mass transport by a climate model. *CGER's Supercomputer Monograph Report*, vol 3. Center for Global Environmental Research, National Institute for Environmental Studies: Tsukuba; 148 pp.
- Ohfuchi W, Nakamura H, Yoshioka MK, Enomoto T, Takaya K, Peng X, Yamane S, Nishimura T, Kurihara Y, Ninomiya 2004. 10-km mesh meso-scale resolving simulations of the global atmosphere on the Earth Simulator: preliminary outcomes of AFES (AGCM for the Earth Simulator). *Journal of the Earth Simulator* **1**: 8–34.
- Sultan B, Janicot S. 2000. Abrupt shift of the ITCZ over West Africa and intra-seasonal variability. *Geophysical Research Letters* **27**: 3353–3356.
- Sultan B, Janicot S. 2003. The West African monsoon dynamics. Part II: The “preonset” and “onset” of the summer monsoon. *Journal of Climate* **16**: 3407–3427.